

Abelian deterministic self organized criticality model: Complex dynamics of avalanche waves.

Jozef Černák*

*P. J. Šafárik University in Košice, Institute of Physics,
Jesenná 5, 04000 Košice, Slovak Republic*

Abstract

The aim of this study is to investigate a wave dynamics and size scaling of avalanches which were created by the mathematical model [J. Černák, Phys. Rev. E **65**, 046141 (2002)]. Numerical simulations were carried out on a two dimensional lattice $L \times L$ in which two constant thresholds $E_c^I = 4$ and $E_c^{II} > E_c^I$ were randomly distributed. A density of sites c with the threshold E_c^{II} and threshold E_c^I are parameters of the model. I have determined autocorrelations of avalanche size waves, Hurst exponents, avalanche structures and avalanche size moments for several densities c and thresholds E_c^{II} . I found correlated avalanche size waves and multifractal scaling of avalanche sizes not only for specific conditions, densities $c = 0.0, 1.0$ and thresholds $8 \leq E_c^{II} \leq 32$, in which relaxation rules were precisely balanced, but also for more general conditions, densities $0.0 < c < 1.0$ and thresholds $8 \leq E_c^{II} \leq 32$, in which relaxation rules were unbalanced. The results suggest that the hypothesis of a precise relaxation balance could be a specific case of a more general rule.

PACS numbers: 45.70.Ht, 05.65.+b, 05.70.Jk, 64.60.Ak

*Electronic address: jcernak@upjs.sk

I. INTRODUCTION

Bak, Tang, and Wiesenfeld (BTW) [1] introduced a concept of self-organized criticality (SOC) to study dynamical systems with spatial degree of freedom. They proposed a simple model with conservative and deterministic relaxation rules to demonstrate the SOC phenomenon. Manna [2] designed another conservative SOC model in which stochastic relaxation rules were defined. Striving to find common features of the models and to know their basic behaviors stimulated many numerical and theoretical studies during the past two decades.

Based on renormalization group calculations, Pietronero *et al.* [3] claimed that both deterministic [1] and stochastic models [2] belong to the same universality class, i.e. a small modification in the relaxation rules cannot change universality class. Chessa *et al.* [4] assumed that finite size scaling (FSS) is common property of both deterministic [1] and stochastic [2] models. With FSS the avalanche size, area, lifetime, and perimeter follow power laws with cutoffs [4]:

$$P(x) = x^{-\tau_x} F(x/L^{D_x}), \quad (1)$$

where $P(x)$ is the probability density function of x , F is the cutoff function, and τ_x and D_x are the scaling exponents. The set of scaling exponents (τ_x, D_x) defines the universality class [4]. A SOC model is *Abelian* if a final stable configuration (see below) does not depend on the relaxation order. The BTW model is *Abelian*, however the M model is also *Abelian* [5] only if we consider probabilities of many stable configurations.

Based on numerical simulations and an extended set of exponents, Ben-Hur and Biham [6] claimed that the BTW and M models cannot belong to the same universality class. A precise numerical analysis of probability density functions $P(x)$ led Lübeck and Usadel [7] to the same conclusion. Essential progress to understand the discrepancy between theoretical [3, 4] and numerical conclusions [6, 7] has been achieved by Tebaldi *et al.* [8]. They found that avalanche size probability density functions $P(s)$ do not display FSS but show a multifractal scaling i.e. the avalanche size exponent τ_s (Eq. 1) does not apply to the BTW model. Karmakar *et al.* [9] proposed a hypothesis that the presence or absence of a precise relaxation balance between the amount released by a site and the total quantity which the same site receives when all its neighbors relax at once determines the appropriate universality class.

Based on the precise relaxation balance hypothesis [9] Karmakar and Manna [10] proposed a flow chart to classify different SOC models into two universality classes i.e. the BTW and Manna universality classes.

The probability density functions of avalanche sizes $P(s)$ in Eq. 1 show transitions from multifractal to FSS scaling for certain densities of disturbing sites [9, 11]. The models [9, 11] are stochastic and *non-Abelian* with unbalanced relaxation rules [9]. In this study, I focus on verifying an existence of such transitions for the deterministic and *Abelian* model [12] (In the original paper [12] the model was incorrectly classified as non-*Abelian*) with unbalanced relaxation rules. The model [12] displays an anomalous increase of the avalanche size area exponents τ_a (Eq. 1) for densities near $c = 0.01$ and thresholds $E_c^{II} \geq 16$. However, the cause of this anomalous behavior is not well understood. I assumed that the transition from multifractal to FSS scaling could take place for density $c < 0.01$ and threshold $E_c^{II} \geq 16$, because relaxation rules change character from balanced ($c = 0.0$) to unbalanced ($c > 0.0$). To characterize avalanche size scaling I investigated avalanche wave dynamics [13, 14], Hurst exponents [13], avalanche structures [6] and avalanche size moments [13].

The paper is organized as follows. In Sec. II I repeat a definition of the inhomogeneous sand pile model [12]. In Sec. III I determine autocorrelations and fluctuations of avalanche size waves, avalanche structures and avalanche size moments for several densities $0.0 \leq c \leq 1.0$ and thresholds $8 \leq E_c^{II} \leq 32$. Sec. IV is devoted to a discussion which is followed by conclusions in Sec. V.

II. AN ABELIAN DETERMINISTIC AND CONSERVATIVE SELF ORGANIZED CRITICALITY MODEL

The inhomogeneous sand pile model [12] is defined on a two dimensional lattice of size $L \times L$. Each site \mathbf{i} has assigned variables $E(\mathbf{i})$ and $E_c(\mathbf{i})$. The variable $E(\mathbf{i})$ is dynamical and it represents a physical quantity such as energy, grain density, and etc. The threshold $E_c(\mathbf{i})$ is a static value at site \mathbf{i} which is defined only once during initialization of simulations. The threshold $E_c(\mathbf{i})$ has two values [12]:

$$E_c(\mathbf{i}) = \begin{cases} E_c^I = 2d \\ E_c^{II} = 2dk, \quad k = 2, 3, 4, \dots, \end{cases} \quad (2)$$

where d is a dimension and k is a natural number. The model has two parameters namely the density $c = n/L^2$ and threshold E_c^{II} where n is a number of sites with the threshold $E_c(\mathbf{i}) = E_c^{II}$, remaining $L^2 - n$ sites have the threshold $E_c^I = 4$. During initializations of simulations, n sites with thresholds $E_c(\mathbf{i}) = E_c^{II}$ were picked out randomly and all remaining sites had the threshold $E_c^I = 4$, thus a set of the thresholds $\{E_c(\mathbf{i})\}$ represents a quenched disorder. A stable configuration is defined by a condition $E(\mathbf{i}) < E_c(\mathbf{i})$ for each site \mathbf{i} . Let us assume that from a stable configuration we iteratively select \mathbf{i} at random and increase $E(\mathbf{i}) \rightarrow E(\mathbf{i}) + 1$. If an unstable configuration is reached i.e. $E(\mathbf{i}) \geq E_c(\mathbf{i})$ then a relaxation starts. The relaxation rules are conservative and deterministic [12]:

$$E(\mathbf{i}) \rightarrow E(\mathbf{i}) - \sum_e \Delta E(\mathbf{e}), \quad (3)$$

$$E(\mathbf{i} + \mathbf{e}) \rightarrow E(\mathbf{i} + \mathbf{e}) + \Delta E(\mathbf{e}), \quad (4)$$

$$\sum_e \Delta E(\mathbf{e}) = E_c(\mathbf{i}), \quad (5)$$

where \mathbf{e} is a set of vectors from the site \mathbf{i} to its neighbors. The relaxation rules (Eqs. 3-5) are repeated until the site \mathbf{i} becomes stable. If the neighbors of the site \mathbf{i} become unstable then avalanche can run on. All unstable sites belong to the avalanche. The relaxations given by Eqs. 3-5 are repeated until a stable configuration is reached, i.e. $E(\mathbf{i}) < E_c(\mathbf{i})$ for all sites \mathbf{i} . Stable and unstable configurations are repeated many times. A total number of relaxations during one avalanche is an avalanche size s .

III. NUMERICAL RESULTS

Numerical simulations were carried out on two dimensional lattices $L \times L$ where the linear lattice size L was $L = 128, 256, 512, 1024, 2048, \text{ and } 4096$. A density c and thresholds $E_c^I = 4, E_c^{II} = 8, 16 \text{ and } 32$ were chosen based on the previous results [12] to cover a

parameter space in which interesting behaviors were expected (Sec. I). For example, near the density $c = 0.01$ an anomalous increase of the avalanche area scaling exponent τ_a (Eq. 1) has been observed [12]. Near densities $c = 0.0$ and 1.0 local relaxation rules change character from balanced ($c = 0.0$ and 1.0) to unbalanced ($c > 0.0$ and $c < 1.0$) [9, 10], thus a transition from multifractal to finite size scaling could take place in the intervals $c > 0.0$ and $c < 1.0$. Considering these assumptions, I have selected the density c as follows: $c = a$ (surroundings of $c = 0.0$) or $c = 1.0 - a$ (surroundings of $c = 1.0$) where $a = 0, 0.001, 0.002, 0.004, 0.008, 0.01, 0.02, 0.04, \text{ and } 0.08$. In addition, to cover the whole interval $0.0 < c < 1.0$, I added the sample concentrations $c = l/10$, where $l = 1, 2, \dots, 9$. I have recorded about 10^6 avalanches after initializations of simulations in which an avalanche dynamics has to reach the SOC state [1]. To qualify a reproducibility of the results all numerical simulations were repeated once for each lattice size $L \times L$, concentration $0.0 \leq c \leq 1.0$ and threshold E_c^{II} . A comparison of these data sets showed that the results are well reproducible.

A possibility to decompose an avalanche into waves [15] is a significant advantage of computer models. Because avalanche wave dynamics [13, 14] can provide valuable initial information about the character of an SOC model. An avalanche of size s is decomposed into m waves with size s_k , where $s = \sum_{k=1}^m s_k$. A time sequence of avalanche waves s_k is used to determine the autocorrelation function [13, 14]

$$C(t, L) = \frac{\langle s_{k+t} s_k \rangle_L - \langle s_k \rangle_L^2}{\langle s_k^2 \rangle_L - \langle s_k \rangle_L^2}, \quad (6)$$

where time is $t = 1, 2, \dots$, and the time averages are taken over 5×10^6 waves. Autocorrelations $C(t, L, c)$ have been analyzed for the time $1 \leq t \leq 1000$, lattice sizes $128 \leq L \leq 4096$, selected concentrations $0.0 \leq c \leq 1.0$ and thresholds $E_c^I = 4, E_c^{II} = 8, 16, \text{ and } 32$ (see above). The autocorrelations $C(t, L = 4096, c)$ for the biggest lattice size $L = 4096$ are shown in Fig. 1. I have observed that for the density $c = 1.0$, the autocorrelations $C(t, L = 4096, c = 1.0)$ agree within experimental error with autocorrelations of the BTW model [13] ($C(t, L = 4096, c = 0.0)$). I note that the autocorrelations $C(t, L = 4096, c = 0.0)$ are not shown in Fig. 1. I have approximated the autocorrelations $C(t, L, c = 0, 1.0)$ by a simple function $C(t, L, c = 0, 1.0) \sim \exp(-\alpha t)$ where α is a decay rate [16]. For more general conditions, densities $0.0 < c < 1.0$ (Fig. 1), the autocorrelations $C(t, L, c)$ are more

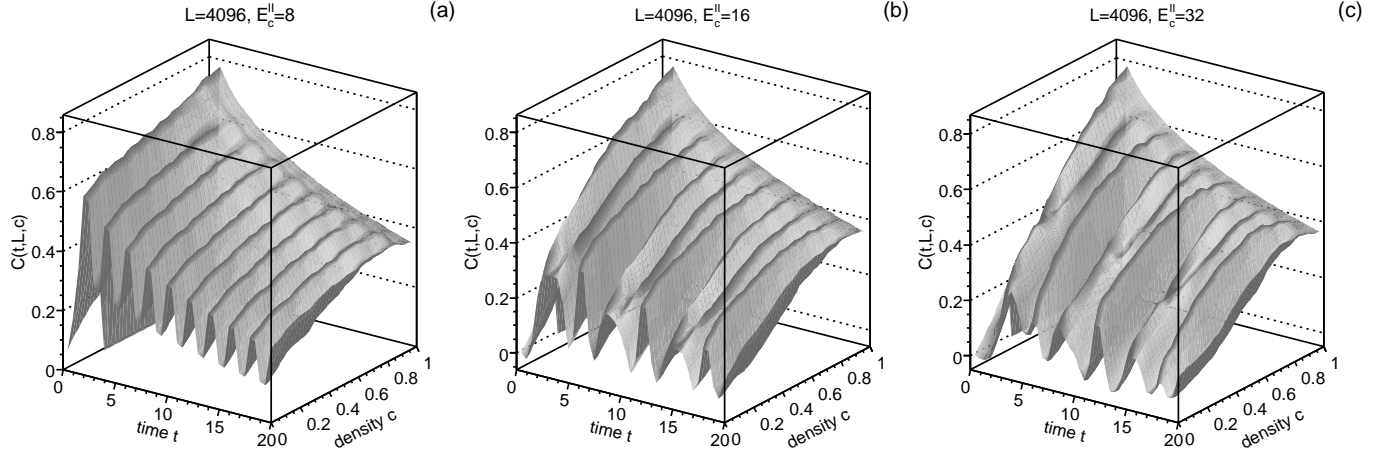


FIG. 1: Autocorrelations $C(t, L, c)$ for the linear lattice size $L = 4096$, for densities $0.001 \leq c \leq 1.0$ and for thresholds $E_c^I = 4$, (a) $E_c^{II} = 8$, (b) $E_c^{II} = 16$, and (c) $E_c^{II} = 32$. The autocorrelations $C(t, L, c = 0)$ are not shown.

complex functions than for specific densities $c = 0.0$ and 1.0 . I have found that with increasing time t , the autocorrelations $C(t, L, c)$ are decreasing functions. An unexpected finding is the existence of oscillating components of autocorrelations. For all densities $0.0 < c < 1.0$ (Fig. 1(a)) and the threshold $E_c^{II} = 8$ their periods are approximately constant. Amplitudes of oscillating components decrease with increasing density c and time t . At the given time t the autocorrelations $C(t, L, c)$ increase if a density c increases, i.e. if $c_2 \geq c_1$ then $C(t, L, c_1) \geq C(t, L, c_2)$. Near densities $c = 0.0$ and 1.0 , the oscillating parts of $C(t, L, c)$ disappear. I have observed more complex behaviors (Fig. 1 (b) and (c)) for thresholds $E_c^{II} \geq 16$ than for the threshold $E_c^{II} = 8$ (Fig. 1 (a)). The oscillating components of $C(t, L, c)$ (Fig. 1(b)) have longer periods for densities $c < 0.08$ and threshold $E_c^{II} = 16$ than for the threshold $E_c^{II} = 8$. However, odd periods were split for densities $c > 0.08$. The same effect take place for the threshold $E_c^{II} = 32$, but a critical density is higher $c \doteq 0.40$ (Fig. 1(c)). After splitting the oscillating components, for thresholds $E_c^{II} = 16$ and 32 , their new periods were approximately equal to the period which has been found for the threshold $E_c^{II} = 8$.

Stochastic processes are often characterized by Hurst exponents [17]. To determine the Hurst exponent the fluctuation $F(t, L)$ [13]:

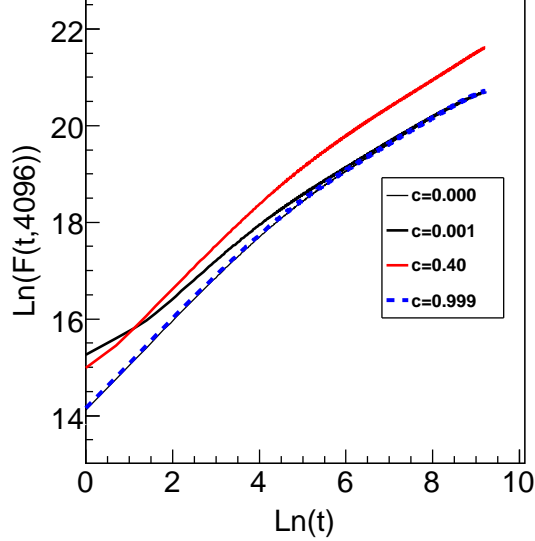


FIG. 2: (Color online) Fluctuations $F(t, L = 4096)$ for densities $c = 0.000, 0.001, 0.40$ and 0.999 and the threshold $E_c^{II} = 32$.

$$F(t, L) = [\langle \Delta y(t)^2 \rangle_L - \langle \Delta y(t) \rangle_L^2]^{1/2} \quad (7)$$

is used where $y(t) = \sum_{k=1}^t s_k$ and $\Delta y(t) = y(k+t) - y(k)$. If a fluctuation $F(t, L)$ scales with the time t as $F(t, L \rightarrow \infty) \sim t^H$ then H is the Hurst exponent.

I have determined fluctuations and the corresponding Hurst exponents for the lattice size $L = 4096$, selected concentrations c (see above) and thresholds $E_c^I = 4, E_c^{II} = 8, 16,$ and 32 . For all these parameters fluctuations show two scaling regions $1 < t_1 < 100$ and $1000 < t_2 < 10000$. The fluctuations $F(t, L)$, for densities $c = 0.000, 0.001, 0.40$ and 0.999 and threshold $E_c^{II} = 32$, are shown in Fig. 2 to demonstrate the existence of two scaling intervals. The Hurst exponents $H_1(c)$ and $H_2(c)$ as functions of density c and threshold E_c^{II} are shown for all parameters (densities $0.0 \leq c \leq 1.0$ and thresholds $8 \leq E_c^{II} \leq 32$) in Fig. 3. I have observed that the exponents $H_1(c)$ and $H_2(c)$ depend on the parameters (density c and threshold E_c^{II}) in a nontrivial manner (Fig. 3). For densities $0.0 \leq c \leq 1.0$ and thresholds $8 \leq E \leq 32$ functions $H_1(c)$ are bounded by the interval $0.68 < H_1(c) < 0.81$. Similarly, the functions $H_2(c)$ are limited by the interval $0.44 < H_2(c) \leq 0.56$. The exponents $H_1(c) \doteq 0.80$ and $H_2(c) \doteq 0.50$ are approximately constant for densities $c > 0.50$. I have observed anomalous decreases of functions $H_{1,2}(c)$ near low densities $0.0 < c \leq 0.01$ (Fig. 3). In addition, functions of $H_{1,2}(c)$ have a decreasing tendency if the second thresholds

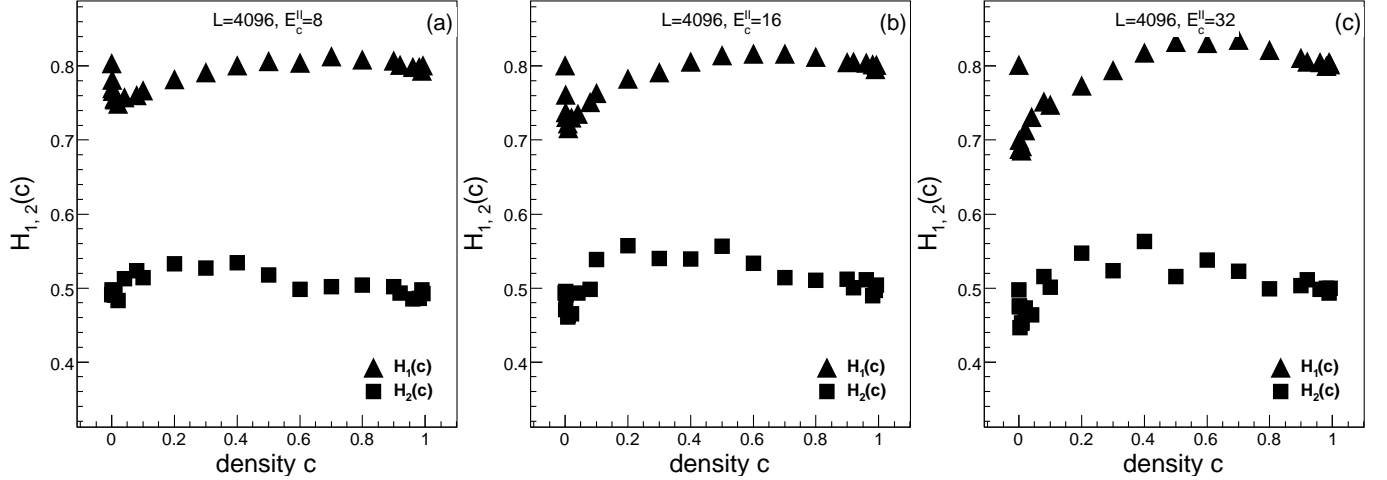


FIG. 3: Hurst exponents $H_1(c)$ and $H_2(c)$ as functions of a densities c and thresholds: $E_c^I = 4$, (a) $E_c^{II} = 8$, (b) $E_c^{II} = 16$, and (c) $E_c^{II} = 32$ for the lattice size 4096×4096 . The Hurst exponents at given density c , $H_1(c)$ and $H_2(c)$ were approximated using the power laws $F(t, L) \sim t^{H_1(c)}$ and $F(t, L) \sim t^{H_2(c)}$ in the intervals $t = 1 - 100$ and $t = 10^3 - 10^4$.

E_c^{II} increase. Finally, the functions $H_{1,2}(c)$ are not symmetric around the density $c = 1/2$, i.e. $H_1(0.5 - a) \neq H_1(0.5 + a)$ and $H_2(0.5 - a) \neq H_2(0.5 + a)$ for $0.0 < a < 0.5$ except the specific densities $c = 0.0$ and $c = 1.0$, where $H_1(0.0) \doteq H_1(1.0)$ and $H_2(0.0) \doteq H_2(1.0)$ within experimental errors.

Ben-Hur and Biham [6] proposed to use avalanche structures to demonstrate a difference between BTW [1] and M [2] models. An avalanche structure consists of clusters of sites with equal numbers of relaxations. The BTW model displays rigorous shell-like structures [6, 9] and the M model displays disordered structures [6] with inner holes [9]. I have analyzed several avalanche structures (Fig. 4) of the inhomogeneous sand pile model [12] to compare them with known structures [6, 9].

I have observed the avalanche structures which resemble the shell-like structure for densities $c = 0.02$ (Fig. 4(a), (d), and (g)) and $c = 0.98$ (Fig. 4 (c), (f), and (i)). However, these structures are not exactly shell-like. A clear visible difference is the existence of holes in an avalanche, for example see Figs. 4(a), (b), and (d). The sizes of these holes vary from one site (obviously a site with $E_c^{II} > E_c^I$) to several sites. Mainly, for low densities ($c = 0.02$) an existence of holes is clearly demonstrated in Figs. 4(a), (d), and (g) where the sites with the threshold E_c^{II} can absorb and relax more energy than surrounding sites with

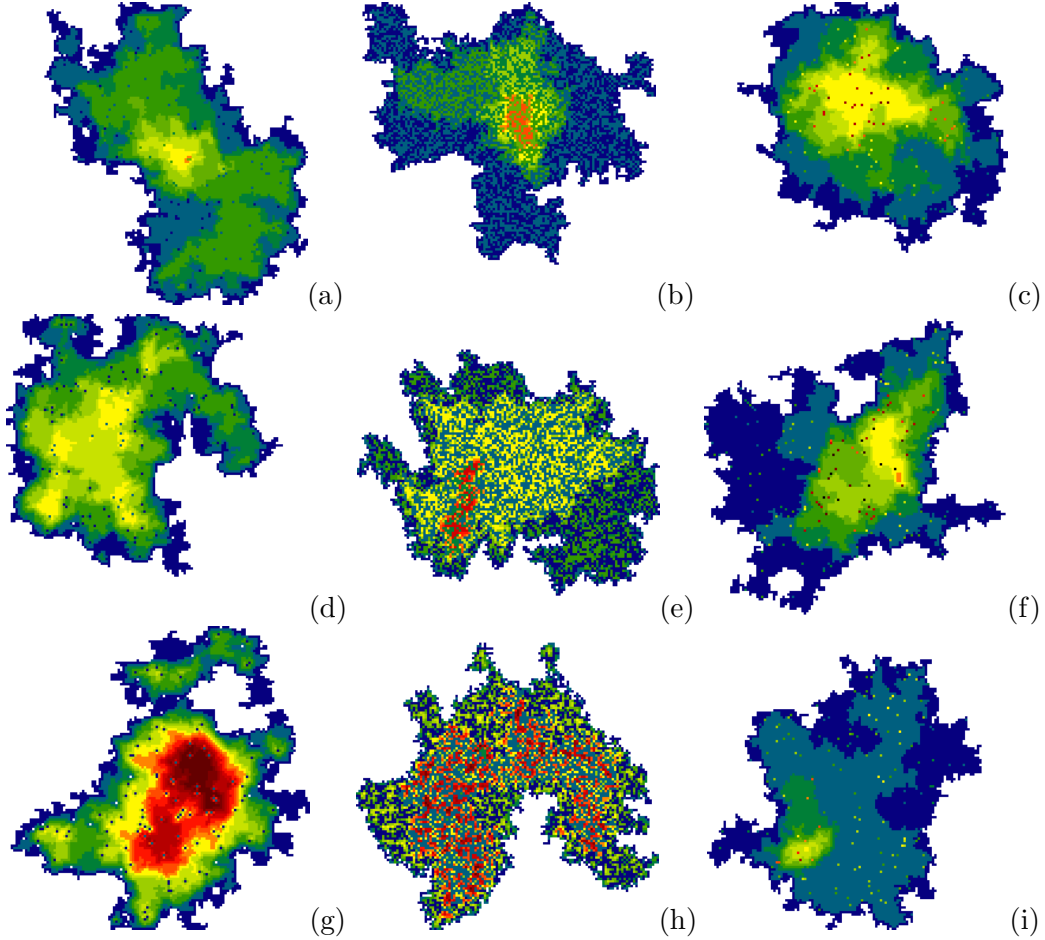


FIG. 4: Avalanche structures on two dimensional lattice 128×128 for parameters $E_c^I = 4$, (a) $E_c^{II} = 8$, $c = 0.02$, (b) $E_c^{II} = 8$, $c = 0.5$, (c) $E_c^{II} = 8$, $c = 0.98$, (d) $E_c^{II} = 16$, $c = 0.02$, (e) $E_c^{II} = 16$, $c = 0.5$, (f) $E_c^{II} = 16$, $c = 0.98$, (g) $E_c^{II} = 32$, $c = 0.02$, (h) $E_c^{II} = 32$, $c = 0.5$, and (i) $E_c^{II} = 32$, $c = 0.98$. Lattice sites with the same numbers of relaxations are shown by the same color (rainbow pseudo-color coding).

E_c^I . If the sites (E_c^{II}) absorb energy then they are well identified as small holes inside the avalanche structure (Figs. 4(a), (d), and (g)). If the sites (E_c^{II}) release more energy than their neighbors (with threshold E_c^I) then the sites (E_c^{II}) involve instabilities of many sites within a certain distance. These sites must relax to be stable (Fig. 4 (d)). At high density $c = 0.98$, the sites with the lower threshold E_c^I are considered for disturbing sites. A site with threshold E_c^I can receive more energy from neighbors than a critical amount of the site (threshold E_c^I). Then the site (E_c^I) must relax more times than neighbors (sites with the threshold E_c^{II}) to be stable. The disturbing sites are shown as isolated sites in Figs. 4(c),

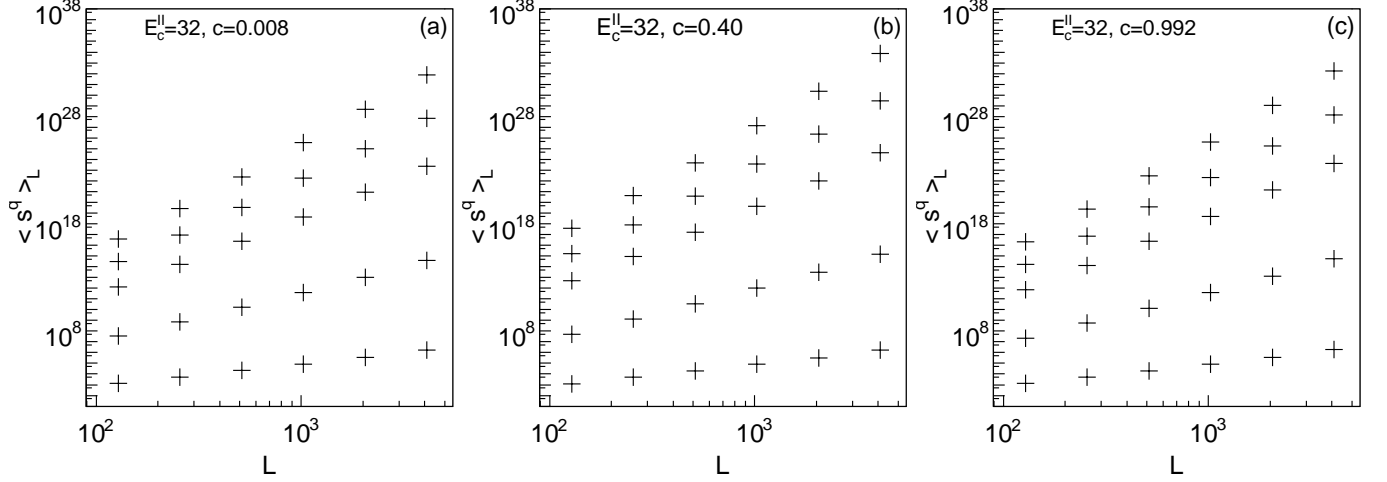


FIG. 5: Scaling of avalanche size moments $\langle s^q \rangle$ versus the lattice size $128 \leq L \leq 4096$. The exponents q are $q = 1.0, 2.0, 3.0, 3.5$ and 3.95 from bottom to top. The model parameters are $E_c^I = 4$, $E_c^{II} = 32$, (a) $c = 0.008$, (b) $c = 0.40$ and (c) $c = 0.992$.

(f), and (i). The effects of disturbing sites E_c^I and E_c^{II} differs, for the small density $c = 0.02$, the disturbing sites E_c^{II} can absorb and relax more energy as their neighbors. However, for high density $c = 0.98$, the disturbing sites E_c^I can only do more relaxations than their neighbors sites.

I have found new avalanche structures which resemble neither shell-like (the BTW mode) nor disordered (the M model) [6, 9] for density $c = 0.50$ and thresholds $8 \leq E_c^{II} \leq 32$ Figs. 4(b), (e), and (h). Their typical feature is the existence of complex clusters in avalanche which more resemble percolation clusters.

The model (Sec. II) displays shell-like avalanche structures as well as the BTW model [6, 9] only for the specific densities $c = 0.0$ and $c = 1.0$.

Sometimes we cannot decompose an avalanche into waves, obviously if we study real systems, then avalanche moments [13] are useful. A property x in FSS obeys scaling given by Eq. 1. The moments q are [13]:

$$\langle x^q \rangle = \int_0^{x_{max}} x^q P(x, L) dx \sim L^{\sigma_x(q)} \quad (8)$$

where $\sigma_x(q) = (q + 1 - \tau_x)D_x$ and $x_{max} \sim L^{D_x}$. I have determined only avalanche size moments $\langle s^q \rangle$ versus the lattice size L which are shown in Fig. 5 for densities $c = 0.008$, $c = 0.40$ and $c = 0.992$ and for thresholds $E_c^I = 4$ and $E_c^{II} = 32$. The moments $\langle s^q \rangle$ scale

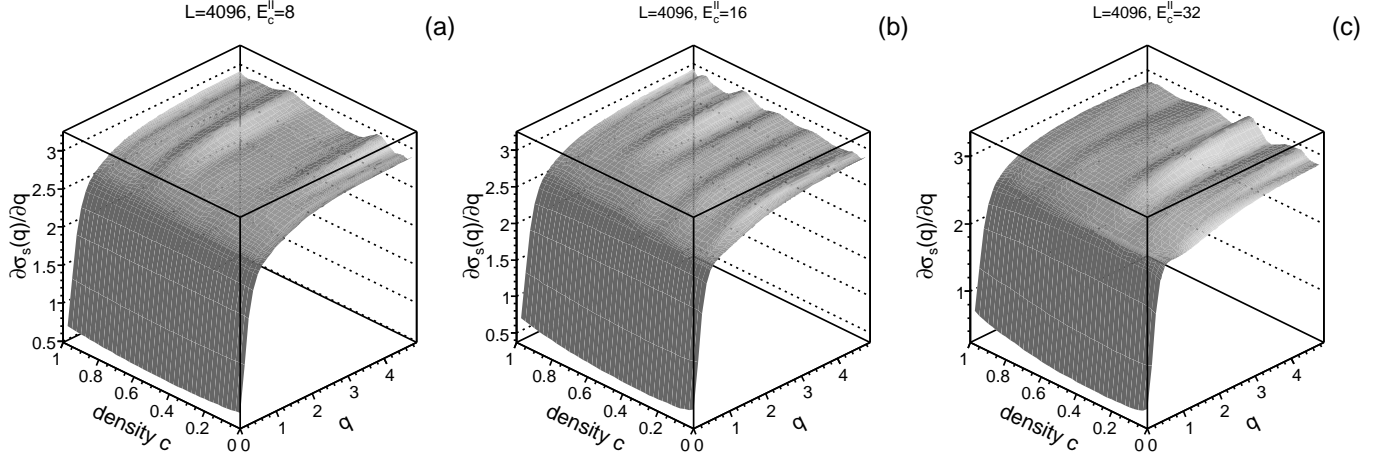


FIG. 6: Plots $\partial\sigma_s(q)/\partial q$ versus exponent q for the lattice size 4096×4096 , concentrations $0.0 < c \leq 1.0$ and thresholds: $E_c^I = 4$, (a) $E_c^{II} = 8$, (b) $E_c^{II} = 16$, and (c) $E_c^{II} = 32$.

with the lattice size L as well as $\langle s^q \rangle \sim L^{\sigma_x(q)}$ (Eq. 8), thus a basic requirement is met to determine $\sigma_s(q)$.

Using the functions $\sigma_s(q)$ I determined the plots $\partial\sigma_s(q)/\partial q$ versus the exponent q which are shown in Fig. 6 for densities $0.0 < c \leq 1.0$ and thresholds $4 < E_c^{II} \leq 32$. I have observed that the functions $\partial\sigma_s(q)/\partial q$ are increasing if exponents q increase (Fig. 6) for exponents $q > 1.0$, densities $0.0 < c < 1.0$ and thresholds $8 \leq E_c^{II} \leq 32$. Surface cuts $\partial\sigma_s(q)/\partial q|_{q=1.0}$ and $\partial\sigma_s(q)/\partial q|_{q=4.0}$, for exponents $q = 1.0$ and $q = 4.0$, as functions of density c are shown in Fig. 7 to demonstrate this increasing tendency. I have found that $\partial\sigma_s(q)/\partial q|_{q=4.0} > \partial\sigma_s(q)/\partial q|_{q=1.0}$, $\partial\sigma_s(q)/\partial q|_{q=1.0} \neq const.$ and $\partial\sigma_s(q)/\partial q|_{q=4.0} \neq const.$ (Fig. 7) for densities $0.0 < c < 1.0$ and thresholds $8 \leq E_c^{II} \leq 32$. This implies that functions $\partial\sigma_s(q)/\partial q$ differ from the function $\partial\sigma_s(q)/\partial q$ of the BTW model. However, for the specific parameters $c = 0.0$, $c = 1.0$ and $8 \leq E_c^{II} \leq 32$ relaxation rules are precisely balances and the functions $\partial\sigma_s(q)/\partial q$ versus q ($q \geq 1.0$) are identical within experimental errors with the function $\partial\sigma_s(q)/\partial q$ of the BTW model [9, 13].

IV. DISCUSSION

I have found that autocorrelations $C(t, L, c)$ (Fig. 1) are more complex functions than an autocorrelation of the BTW model [9, 13]. The autocorrelations exhibit oscillating components (Fig. 1) which periods and amplitudes depend on both densities $0.0 < c < 1.0$ and

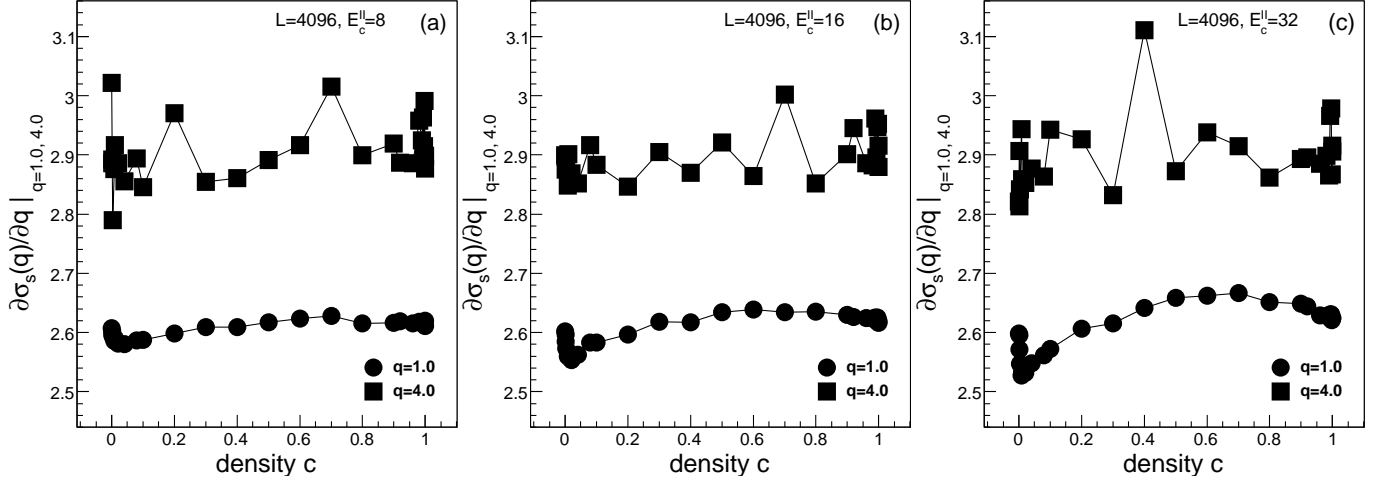


FIG. 7: The plots $\partial\sigma_s(q)/\partial q|_{q=1}$ (errors ± 0.01) and $\partial\sigma_s(q)/\partial q|_{q=4}$ (errors ± 0.03) versus density c for the linear lattice size $L = 4096$ and thresholds $E_c^I = 4$, (a) $E_c^{II} = 8$, (b) $E_c^{II} = 16$, and (c) $E_c^{II} = 32$.

thresholds $8 \leq E_c^{II} \leq 32$. The oscillating components are probably caused by a periodicity in an avalanche wave sequence. I assume that the periodicity could be a consequence of an excessive energy storing and release in sites with the thresholds E_c^{II} , apparently when the sites have low concentration $c < 0.5$. In such conditions, relaxations of these sites trigger relaxations of surrounding sites, i.e. all surrounding sites within a certain distance from a disturbing site have to relax [12]. This hypothesis could be supported by finding that for the same time t amplitudes of oscillating components are decreasing if densities c increase and oscillations disappear near the density $c = 1.0$ (Fig. 1). The periods were longer for low densities $c < 0.4$ and thresholds $E_c^{II} \geq 16$ than for the threshold $E_c^{II} = 8$. This could be connected with the stronger effect of disturbing sites $E_c^{II} \geq 16$ which can store and release much more energy than disturbing sites $E_c^{II} = 8$. However, a nontrivial dependence of periods on thresholds $E_c^{II} \geq 8$ and densities c (Fig. 1) and the cause of period splitting for thresholds $E_c^{II} \geq 16$ and critical densities c (Fig. 1 (b) and (c)) are not understood. For specific densities $c = 0.0$ and $c = 1.0$, the autocorrelations $C(t, L, c = 0.0)$ and $C(t, L, c = 1.0)$ agree well with autocorrelation of the BTW model [9, 13]. I have found correlated avalanche waves under more general conditions in which the relaxation rules are unbalanced [9] for densities $0.0 < c < 1.0$ and thresholds $8 \leq E_c^{II} \leq 32$. This is completely opposite to the result the hypothesis predicted [9, 10]. I think that the hypothesis about a precise relaxation

balance [9, 10] is valid only for the specific densities $c = 0.0$ and $c = 1.0$ and thresholds $8 \leq E_c^{II} \leq 32$.

Two scaling intervals of fluctuations $F(t, L = 4096)$ (Fig. 3) support correlated avalanche waves [13] for densities $0.0 \leq c \leq 1.0$ and thresholds $8 < E_c^{II} \leq 32$. The fluctuations $F(t, L = 4096)$ agree well with a fluctuation of the BTW model only for the densities $c = 0.0$ and $c = 1.0$ [9, 13] when relaxation rules are precisely balanced [9]. For all other parameters, densities $0.0 < c < 1.0$ and thresholds $8 \leq E_c^{II} \leq 32$, relaxation rules are unbalanced and the hypothesis [9, 10] predicts a single scaling region with the Hurst exponent $H = 1/2$. However, I have not found single scaling regions of $F(t, L = 4096)$. So the fluctuations $F(t, L = 4096)$ contradict the hypothesis of precise relaxation balance [9, 10]. Asymmetries of functions $H_{1,2}(c)$ to permutations of densities c (Fig. 3) could be a consequence of different local effects of disturbing sites E_c^{II} near density $c = 0.0$ and disturbing sites E_c^I near density $c = 1.0$. The Hurst exponents $H_1(c)$ are limited by the interval $0.68 < H_1(c) < 0.8$ near the density $c = 0.0$ thus avalanche waves are less correlated than in the BTW model ($H_1 = 0.8$) and they are more correlated than in the M model ($H = 0.5$). The Hurst exponents $H_2(c)$ are limited by the interval $0.44 < H_2(c) \leq 0.56$ which indicate that local perturbation effects can change a long-term persistence (antipersistence) [17]. The changes of Hurst exponents $H_{1,2}(c)$ with density c and threshold E_c^{II} demonstrate that local perturbation effects could change a global wave dynamics.

I assume that avalanche wave dynamics (autocorrelations and fluctuations) on a finite size lattices $L \times L$, for $L > L_c$ where L_c is a critical length, can provide basic information about correlated (the BTW model) or uncorrelated (the M model) nature of waves in avalanches not only for the finite size L but also for the size L which goes to infinity. I assume that $L = 4096$ is greater than L_c . Then conclusions regarding an avalanche wave dynamics for the finite lattice size $L = 4096$ could be extended for infinite systems.

A comparison of avalanche structures, for densities $0.0 < c < 1.0$ and thresholds $8 \leq E_c^{II} \leq 32$, shows that the avalanche structures of the model (Sec. II) are more disordered than shell-like structures of the BTW [6, 9] model but they are more ordered than structures of the M model [6, 9]. Only for the specific densities $c = 0.0$ and $c = 1.0$, the avalanche structures are exactly shell-like as well as in the BTW model [6, 9]. I assume that connection between avalanche structures and autocorrelations near the density $c = 0.5$ are more weak for the model (Sec. II) than for the BTW or M models [6, 9]. Because avalanche structures

are more disordered (Fig. 4) than structures of the BTW model and more ordered than structures of the M model, however avalanche waves are correlated as in Fig. 1.

A hypothesis about a precise relaxation balance [9] for unbalanced relaxation rules predicts FSS where $\partial\sigma_s(q)/\partial q = \text{const.}$ for all exponents $q > 1.0$. In such case, an expectation $\partial\sigma_s(q)/\partial q|_{q=4} \doteq \partial\sigma_s(q)/\partial q|_{q=1}$ is correct. However, avalanche size moments do not support this expectation, because I have found that $\partial\sigma_s(q)/\partial q|_{q=4} > \partial\sigma_s(q)/\partial q|_{q=1}$ and functions $\partial\sigma_s(q)/\partial q|_{q=4}$ and $\partial\sigma_s(q)/\partial q|_{q=1}$ (Fig. 7) depend on a density c for all densities $0.0 < c < 1.0$ and thresholds $8 \leq E_c^{II} \leq 32$. This is a reason why functions $\partial\sigma_s(q)/\partial q$ of the model (Sec. II) cannot be identical with the function $\partial\sigma_s(q)/\partial q$ of the BTW model [2, 9] ($c = 0.0$ and 1.0) for densities $0.0 < c < 1.0$. Although, I conclude that avalanche waves are correlated in avalanches and avalanche sizes scale as a multifractal for all investigated parameters.

For specific densities $c = 0.0$ and 1.0 , the basic assumptions $H_i - H'_i = 0$ of the precise relaxation balance hypothesis [9] are correct. However, all results (Sec. III) show a multifractal scaling of avalanche sizes not only for the specific conditions but also for the more general conditions $0.0 < c < 1.0$ and $8 \leq E_c^{II} \leq 32$ in which $|H_i - H'_i| = 4n$, $0 \leq n \leq 7$ where n is a natural number. Thus I conclude that the hypothesis about precise relaxation balance [9] is valid only for the specific parameters $c = 0.0$ and 1.0 and $E_c^{II} > 4$.

I have not observed a transition from multifractal scaling to FSS of avalanche sizes which has been expected for low densities near $c = 0.0$ (Sec. I). However, the autocorrelations, Hurst exponents and avalanche size moments support the previous conclusions [11, 12, 16] that multifractal scaling is very sensitive to local perturbations for densities near $c = 0.0$.

Does the model belong to the BTW class? The answer is not uniform. The model shows common features with the BTW model for example, correlated waves in avalanches and multifractal scaling of avalanche sizes. However, I have demonstrated that the autocorrelations (Fig. 1) are complex functions, Hurst exponents are functions of densities c (Fig. 3) and holes can be found in avalanches while all these features are not typical for the BTW model. A possible difference between the inhomogeneous sand pile model [12] and the BTW model [1] is supported by functions $\partial\sigma_s(q)/\partial q$ (Figs. 6 and 7) which are not identical with the function $\partial\sigma_s(q)/\partial q$ of the BTW model except the specific densities $c = 0.0$ and 1.0 .

V. CONCLUSION

Applying the classification scheme [10] on the inhomogeneous sandpile model (Sec. II) places the model in the M universality class. However, I have demonstrated (Sec. III) that the model belongs neither in the M universality class nor in the BTW universality class (Sec. IV). I assume that it belongs in a multifractal universality class [8] which is more general than the BTW class [16]. Based on the wave autocorrelations, fluctuations, avalanche structures and avalanche size moments, I conclude that an avalanche wave dynamics and avalanche size scaling depend on local relaxation details. In addition, a hypothesis about precise relaxation balance [9, 10] could be a specific case of a more general rule. The reason why a multifractal scaling is very sensitive to local perturbations is not well understood.

Acknowledgments

The author thanks A. Read for his comments to the manuscript. Computer simulations were carried out in the projects NorduGrid and KnowARC. This work was supported by Slovak Research and Development Agency under contact No. RP EU-0006-06.

-
- [1] P. Bak, C. Tang, and K. Wiesenfeld, *Phys. Rev. Lett.* **59**, 381 (1987).
 - [2] S. S. Manna, *J. Phys. A* **24**, L363 (1991).
 - [3] L. Pietronero, A. Vespignani, and S. Zapperi, *Phys. Rev. Lett.* **72**, 1690 (1994).
 - [4] A. Chessa, H. E. Stanley, A. Vespignani, and S. Zapperi, *Phys. Rev. E* **59**, R12 (1999).
 - [5] Dhar, *Physica A* **270**, 69 (1999).
 - [6] A. Ben-Hur and O. Biham, *Phys. Rev. E* **53**, R1317 (1996).
 - [7] S. Lübeck and K. Usadel, *Phys. Rev. E* **55**, 4095 (1997).
 - [8] C. Tebaldi, M. De Menech, and A. L. Stella, *Phys. Rev. Lett.* **83**, 3952 (1999).
 - [9] R. Karmakar, S. S. Manna, and A. L. Stella, *Phys. Rev. Lett.* **94**, 088002 (2005).
 - [10] R. Karmakar and S.S. Manna, *Phys. Rev. E* **71**, 015101(R) (2005).
 - [11] J. Černák, *Phys. Rev. E* **73**, 066125 (2006).
 - [12] J. Černák, *Phys. Rev. E* **65**, 046141 (2002).

- [13] M. de Menech and A.L. Stella, Phys. Rev. E **62**, R4528 (2000).
- [14] A. L. Stella and M. de Menech, Physica A **295**, 101 (2001).
- [15] E. V. Ivashkevich, D.V. Ktitarev, and V. B. Priezzhev, Physica A **209**, 347 (1994).
- [16] J. Černák, arXiv:0807.4113v2 [cond-mat.stat-mech].
- [17] Benoit B. Mandelbrot, *The fractal geometry of nature* (W. E. Freeman and Company, New York, 1983).